LETTER

doi:10.1038/nature21702

The allosteric inhibitor ABL001 enables dual targeting of BCR–ABL1

Andrew A. Wylie[1], Joseph Schoepfer[2], Wolfgang Jahnke[2], Sandra W. Cowan-Jacob[2], Alice Loo[1], Pascal Furet[2], Andreas L. Marzinzik[2], Xavier Pelle[2], Jerry Donovan[1], Wenjing Zhu[1], Silvia Buonamici[1]†, A. Quamrul Hassan[1], Franco Lombardo[1], Varsha Iyer[2], Michael Palmer[1], Giuliano Berellini[1], Stephanie Dodd[1], Sanjeev Thohan[1], Hans Bitter[1], Susan Branford[3], David M. Ross[4], Timothy P. Hughes[5], Lilli Petruzzelli[1], K. Gary Vanasse[1], Markus Warmuth[1]†, Francesco Hofmann[2], Nicholas J. Keen[1] & William R. Sellers[1]

Chronic myeloid leukaemia (CML) is driven by the activity of the BCR–ABL1 fusion oncoprotein. ABL1 kinase inhibitors have improved the clinical outcomes for patients with CML, with over 80% of patients treated with imatinib surviving for more than 10 years[1]. Second-generation ABL1 kinase inhibitors induce more potent molecular responses in both previously untreated and imatinib-resistant patients with CML[2]. Studies in patients with chronic-phase CML have shown that around 50% of patients who achieve and maintain undetectable BCR–ABL1 transcript levels for at least 2 years remain disease-free after the withdrawal of treatment[3,4]. Here we characterize ABL001 (asciminib), a potent and selective allosteric ABL1 inhibitor that is undergoing clinical development testing in patients with CML and Philadelphia chromosome-positive (Ph^+) acute lymphoblastic leukaemia. In contrast to catalytic-site ABL1 kinase inhibitors, ABL001 binds to the myristoyl pocket of ABL1 and induces the formation of an inactive kinase conformation. ABL001 and second-generation catalytic inhibitors have similar cellular potencies but distinct patterns of resistance mutations, with genetic barcoding studies revealing pre-existing clonal populations with no shared resistance between ABL001 and the catalytic inhibitor nilotinib. Consistent with this profile, acquired resistance was observed with single-agent therapy in mice; however, the combination of ABL001 and nilotinib led to complete disease control and eradicated CML xenograft tumours without recurrence after the cessation of treatment.

A series of small molecules was previously shown to bind to the BCR–ABL1 myristoyl pocket and inhibit kinase activity via an allosteric mechanism[5]. Unfortunately, these molecules had limited potency and lacked activity against the BCR–ABL1 Thr315Ile mutation[5]. To develop new small molecule scaffolds, we performed fragment-based nuclear magnetic resonance (NMR) screens and optimized resulting hits using *in silico* docking, crystallography and NMR studies. Myristoyl-pocket binders such as GNF-2 must induce a crucial 'bend' in the C-terminal helix to induce the auto-inhibited kinase conformation[6]. Using a conformational NMR assay, molecules with this property from the new series were selected and optimized to improve potency, selectivity and *in vivo* pharmacokinetics, leading to the identification of ABL001 (Fig. 1a and Extended Data Fig. 1a). NMR and biophysical studies confirmed that ABL001 binds potently (dissociation constant (K_d) = 0.5–0.8 nM) and selectively to the myristoyl pocket of ABL1 and induces the inactive C-terminal helix conformation (Extended Data Fig. 1b–d). Comparisons of ABL1 co-crystal structures bound to myristate or ABL001 revealed almost identical binding poses (Fig. 1a). Hence, ABL001 binding mimics the structural consequences of myristate binding to the N terminus of ABL1. Consistent with this binding site, ABL001 exhibits the same non-ATP-competitive biochemical kinetics as the BCR–ABL inhibitor GNF-2 (refs 5, 7) but with approximately 100-fold greater potency (Fig. 1b). Myristoyl-binding sites analogous to that of ABL1 are only found in a limited number of kinases such as SRC[8,9]. Indeed, studies revealed that ABL001 lacks activity against more than 60 kinases, including SRC (Extended Data Table 1a), and is similarly inactive against G-protein-coupled receptors, ion channels, nuclear receptors and transporters (Extended Data Table 1b).

In BCR–ABL1-transformed Ba/F3 cells grown without IL-3, ABL001 had an anti-proliferative half-maximum inhibitory concentration (IC_{50}) value of 0.25 nM. By contrast, the addition of IL-3 to bypass BCR–ABL1 dependence renders these cells insensitive to ABL001 (Extended Data Fig. 2a). In the CML blast-phase cell line KCL-22, ABL001 inhibited phosphorylation of both STAT5 (Tyr694; pSTAT5) and BCR–ABL1 (Tyr245; pBCR–ABL1) after 1 h using concentrations that correlate with those required for inhibition of cell proliferation (Extended Data Fig. 2b, c). Notably, in contrast to nilotinib and dasatinib, ABL001 did not affect the phosphorylation of CRKL (Tyr207) after a short-term 1 h treatment. The cellular activities of ABL001, GNF-2 and a set of clinically approved catalytic-site inhibitors were determined in 450 cancer cell lines from the Cancer Cell Line Encyclopedia[10] (Fig. 1c). ABL001 was selectively active against all BCR–ABL1 lines (IC_{50} value of 1–20 nM), irrespective of the presence of either the p210 or the p190 BCR–ABL1 isoform. GNF-2 was also selective for BCR–ABL1 cell lines but was around 100-fold less potent. Imatinib, nilotinib, dasatinib, bosutinib and ponatinib were active against cell lines containing BCR–ABL1 fusions but varied considerably in their specificity (Fig. 1c).

ABL001 has moderate oral absorption, volume of distribution and half-life across all species (Extended Data Fig. 3a). The pharmacokinetic/pharmacodynamic relationship and *in vivo* efficacy of ABL001 was tested using xenografts derived from the KCL-22 cell line and from patients with Ph^+ acute lymphoblastic leukaemia (ALL). Single doses of 7.5, 15 and 30 mg kg^{-1} ABL001, administered to mice bearing KCL-22 xenografts, inhibited pSTAT5 (Tyr694), which returned to baseline at 10, 12 and 16–20 h after administration of the dose, respectively (Extended Data Fig. 3b). In mice implanted with KCL-22 tumours, the minimum dose of ABL001 required for complete regression was 7.5 mg kg^{-1} twice a day (BID) or 30 mg kg^{-1} once a day (QD), and was tolerated at doses up to 250 mg kg^{-1} BID (Extended Data Fig. 3c, e). Similarly, in xenografts derived from patients with Ph^+ ALL, treatment with 7.5 and 30 mg kg^{-1} ABL001 led to regressions that were maintained during dosing (Extended Data Fig. 3d).

ABL001 was developed to test the hypothesis that the dual inhibition of BCR–ABL1 using distinct targeting mechanisms might improve treatment outcomes by providing enhanced target coverage

[1]Novartis Institutes for BioMedical Research, Cambridge, Massachusetts 02139, USA. [2]Novartis Institutes for BioMedical Research, Basel, Switzerland. [3]Centre for Cancer Biology, SA Pathology and University of South Australia, Adelaide, South Australia 5000, Australia. [4]Haematology Directorate, SA Pathology, PO Box 14, Rundle Mall, Adelaide, South Australia 5000, Australia. [5]South Australian Health & Medical Research Institute (SAHMRI), North Terrace, Adelaide, South Australia 5000, Australia. †Present addresses: H3 Biomedicine Target Biology, 300 Technology Square, Cambridge, Massachusetts 02139, USA.

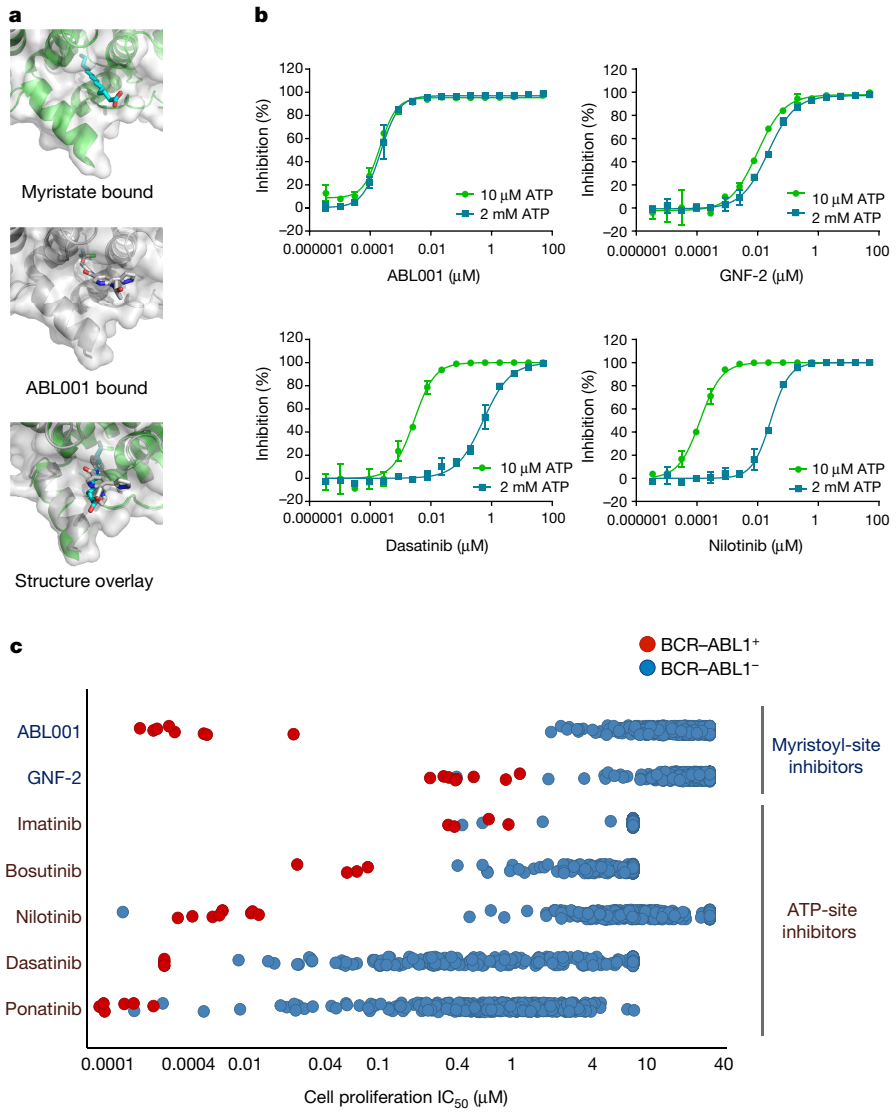

Figure 1 | ABL001 is an allosteric inhibitor of BCR–ABL1 that selectively inhibits growth of BCR–ABL1-driven cells. a, The structure of ABL1 (green) in complex with myristate (cyan), with the transparent surface in grey (Protein Data Bank (PDB) entry 1OPK), the structure of ABL1 (grey) in complex with ABL001 (white) and an overlay of the two images. **b**, Biochemical ABL1 kinase assay at high (2 mM) and low (10 μM) ATP concentrations in the presence of ABL001, GNF-2, nilotinib and dasatinib. Duplicate measurements were taken, and data are mean ± s.d. **c**, Anti-proliferative activity of ABL001, GNF-2, nilotinib, imatinib, dasatinib, bosutinib and ponatinib across a large cancer cell line panel. Cell lines that contain a BCR–ABL1 oncogenic fusion gene are highlighted in red, and the remaining cell lines are highlighted in blue. (Note that the lowest concentration of dasatinib tested was 0.003 μM.)

and preventing the emergence of resistance. Crystallography studies showed that ABL001 and nilotinib can co-bind a single molecule of BCR–ABL1 (Fig. 2a), and *in vitro* studies revealed additive effects of ABL001 in combination with imatinib, nilotinib or dasatinib (Extended Data Fig. 2d). Preventing the emergence of resistance probably depends on two molecules having mechanisms of resistance that do not overlap. ABL001-resistant KCL-22 cells were sequenced and identified as having mutations in the myristoyl pocket and at the interface between the SH3 and kinase domains (Fig. 2b). No inhibitor-resistant catalytic-site mutations were identified. These mutations were functionally validated using Ba/F3 cells engineered to express BCR–ABL1 containing individual ABL001-resistant or catalytic-site-resistant mutations[11]. ABL001 was active in the low nanomolar concentration range against all catalytic-site mutations, including Thr315Ile, whereas catalytic-site inhibitors were active against all ABL001-resistant mutations (Fig. 2c). Clonally derived KCL-22 cells containing either a Thr315Ile or an Ala337Val mutation were tested for their sensitivity to ABL001 or nilotinib (Extended Data Fig. 4a). Nilotinib was inactive against KCL-22 Thr315Ile cells but retained full activity against KCL-22 Ala337Val cells. By contrast, ABL001 was inactive against KCL-22 Ala337Val cells but retained activity against Thr315Ile cells at low nanomolar concentrations readily achieved *in vivo* (Extended Data Fig. 3b). Indeed, ABL001 treatment led to tumour regression of KCL-22 Thr315Ile xenografts at doses of 30 mg kg^{-1} BID (Extended Data Fig. 4b), well below the 250 mg kg^{-1} BID maximum tolerated dose in mice (Extended Data Fig. 3e). A combination of myristoyl-site and catalytic-site inhibitors is therefore likely to create a barrier to the development of mutation-driven acquired resistance.

To explore this possibility further, KCL-22 cells were transduced with a barcode library, in which cells labelled with individual barcodes are tracked under drug treatment. This technique enables the determination of the frequency with which resistant clones emerge and whether such clones pre-exist in a cell population[12]. Barcoded KCL-22 cells were treated with DMSO, ABL001 or nilotinib. Concentration ranges were selected to represent the compound concentration tenfold above their respective KCL-22 anti-proliferative IC_{50} value (10 nM ABL001, 300 nM nilotinib) and the concentration readily achieved clinically (100 nM and 1,000 nM ABL001 (ref. 13), 1,700 nM nilotinib[14]).

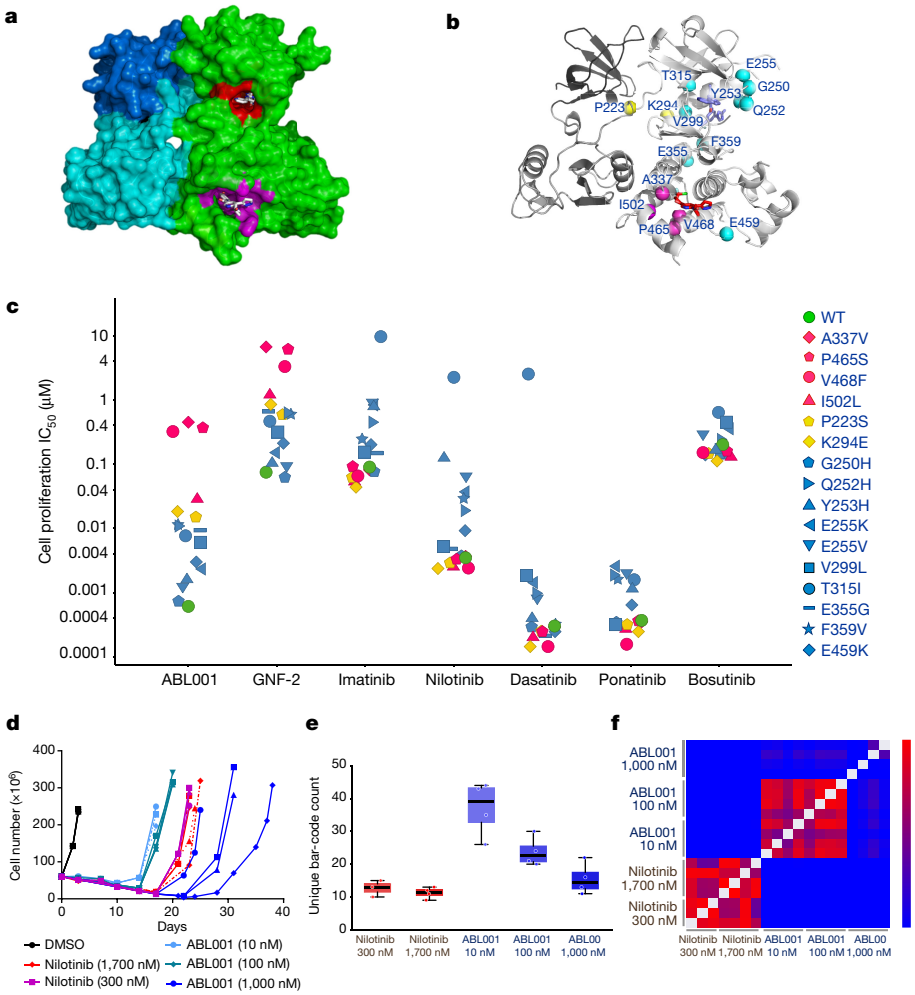

Figure 2 | ABL001 has a resistance profile that is distinct from catalytic-site BCR–ABL1 inhibitors. a, X-ray crystal structure of ABL001 bound to the myristoyl pocket (magenta) and nilotinib bound to the ATP-pocket (red) co-crystallized in a ternary complex with ABL1 (Thr334Ile, Asp382Asn). Green, catalytic domain; dark blue, SH3; light blue, SH2. **b**, Location of resistance mutations overlaid on the ABL1 structure. ABL001-resistant mutations located at the myristoyl site are highlighted in magenta, and those located at the SH3/kinase domain interface are highlighted in yellow. Resistance mutations reported for catalytic-site inhibitors are highlighted in blue. **c**, Ba/F3 cells transformed by BCR–ABL1 containing single point mutations were tested for their sensitivity to ABL001, imatinib, nilotinib, dasatinib, ponatinib and bosutinib in two independent 48 h proliferation assays, and the average IC_{50} values are plotted. Ba/F3 cell lines expressing BCR–ABL1 with ABL001-resistant mutations close to the myristoyl site are in magenta, and those located at the SH3/kinase domain interface are in yellow. Ba/F3 cell lines expressing BCR–ABL1-containing mutations reported to be resistant to catalytic-site inhibitors are in blue. **d**, Approximately 60×10^6 KCL-22 ClonTracer cells were incubated with ABL001 or nilotinib and monitored over time for the outgrowth of resistant cell populations. Each line represents individual replicates (1–4). **e**, The number of unique barcodes present in each resistant population was calculated. A unique barcode is defined as a barcode that is present in the cell population at a frequency higher than 0.57%, which was the highest single barcode frequency found in untreated (DMSO) samples. **f**, The correlation of unique barcodes between different replicates (1–4) and treatment groups is plotted in a heatmap, with barcodes that have a high correlation between treatment groups coloured in red.

Resistance to ABL001 at 10 and 100 nM emerged at day 15, followed by resistance to nilotinib at 300 and 1,700 nM at day 20 (Fig. 2d). In each case, all four replicates for each treatment group developed resistance simultaneously. By contrast, resistance to 1,000 nM ABL001 was the slowest to develop and emerged at varying time points, with one replicate developing resistance at day 20 and other replicates emerging from days 25 to 30. Analysis of the barcodes revealed that nilotinib-resistant clones were derived from cells labelled with 10–15 unique barcodes irrespective of the dose, whereas increasing concentrations of ABL001 led to a dose-dependent reduction in the average number of unique barcodes ranging from around 40 unique barcodes with 10 nM ABL001 to less than 15 unique barcodes with 1,000 nM ABL001 (Fig. 2e). We then compared the barcode profiles across all replicates and treatments to establish the correlations between each resistant population (Fig. 2f). The 300 and 1,700 nM nilotinib-resistant barcodes were highly correlated with each other and did not correlate with the ABL001 barcode profiles. Likewise, although barcode profiles were highly correlated between the 10 nM and 100 nM ABL001-resistant cells, there was no correlation with nilotinib-resistant cells. These data suggest that resistant clones exist before treatment and more importantly, such clones display no shared resistance between the two inhibitors. Interestingly, cells resistant to 1,000 nM ABL001 have unique barcode profiles not only across all other treatment arms but also across each replicate. This may represent a higher selection pressure that either restricts the emergence of resistant cells to those that have acquired *de novo* mutations or, alternatively, allows the emergence of pre-existing mutations that are out-competed by other resistant cells at lower doses.

The complementary resistance profiles of ABL001 and nilotinib suggests that the combination might delay resistance and have a more durable effect than either agent alone. Treatment of KCL-22 xenografts with ABL001 or nilotinib as single agents led to rapid tumour regression (Fig. 3a); however, resistance emerged due to Thr315Ile mutations

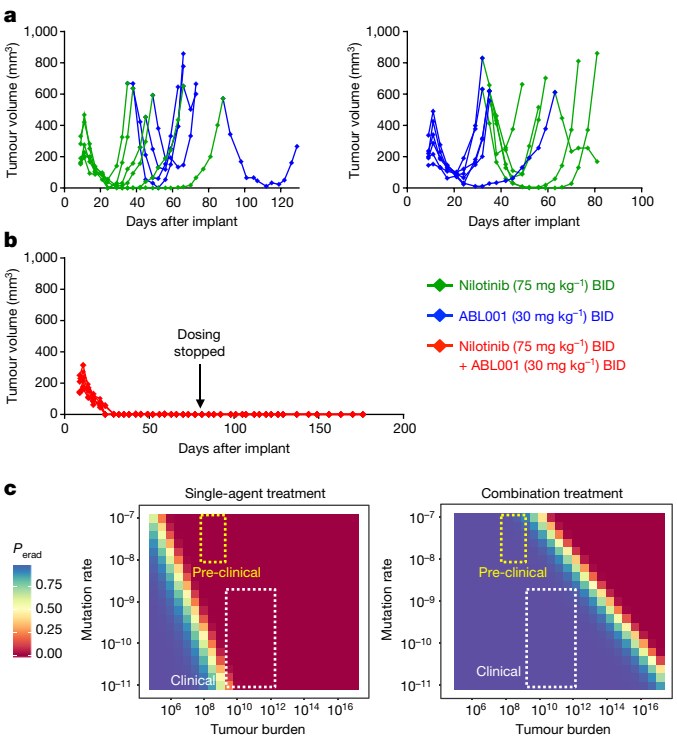

Figure 3 | The non-overlapping resistance profiles of ABL001 and nilotinib enable durable tumour eradication when used in combination. a, KCL-22 mouse xenografts were dosed with 75 mg kg^{-1} BID nilotinib (green) or 30 mg kg^{-1} BID ABL001 (blue), and tumour size was monitored. Each line represents an individual animal. When relapsed tumours grew to more than 500 mm^3, fine needle biopsies were taken for mutational analysis, dosing was switched to the opposite single-agent treatment and tumour size was monitored. **b**, KCL-22 mouse xenografts were treated with a combination of 30 mg kg^{-1} BID ABL001 and 75 mg kg^{-1} BID nilotinib (red) and tumour size was monitored. Each line represents an individual animal. Treatment was stopped on day 77 and tumour growth was monitored for a further 100 days. **c**, Probability of tumour eradication (P_{erad}) when ABL001 and nilotinib are given as single agents or as a combination of agents with mutation profiles that do not overlap, based on the mathematical model described previously[20]. Dashed boxes (yellow) denote estimated pre-clinical KCL-22 tumour burdens and mutational rates; dashed boxes (white) denote estimated clinically relevant tumour burdens and mutational rates. See Supplementary Methods for other parameters (growth, birth and death rates) used in the model.

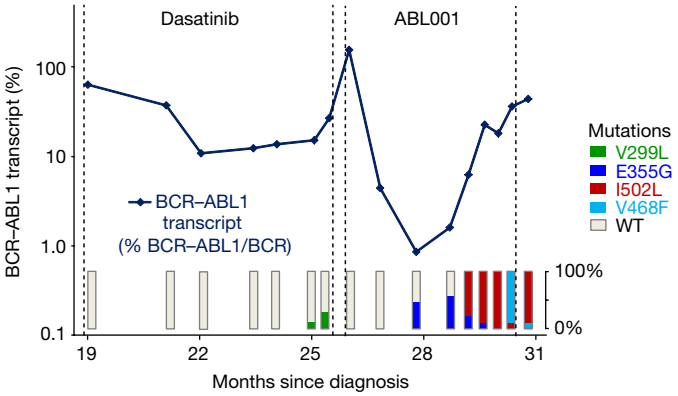

Figure 4 | Clonal evolution of resistance mutations in a patient treated with ABL001 after previous dasatinib treatment. BCR–ABL1 transcript profile and identification of resistant clones in a patient from the start and then discontinuation of treatment with dasatinib, through to treatment with ABL001 and then disease relapse with disease-causing myristoyl-site mutations. Disease burden was monitored using a reverse transcription PCR (RT–PCR) assay that quantifies the relative abundance of *BCR–ABL1* transcripts to *BCR* transcripts (% *BCR–ABL1*/*BCR*) in the peripheral blood. The emergence of resistant clones with point mutations in the BCR–ABL1 kinase domain was determined via sequencing of *BCR–ABL1* transcripts, and their relative abundance to wild-type (WT) *BCR–ABL1* was calculated.

under treatment with nilotinib and Ala337Val or Pro223Ser mutations under treatment with ABL001. Upon outgrowth of the resistant tumours, dosing was switched to the other agent and the tumours regressed once more, suggesting non-cross-resistance. However, this second response was only transient and a second relapse occurred (Fig. 3a). In parallel, tumour-bearing mice were treated upfront with the combination of ABL001 and nilotinib. In contrast to sequential single-agent treatment, the combination led to durable complete regressions in all animals (Fig. 3b). Dosing was stopped after 10 weeks and no evidence of tumour re-growth was observed after an additional 3 months. These data raise the possibility that dual inhibition of BCR–ABL1 might lead to disease eradication and treatment-free remissions.

To assess the clinical translatability of these observations, the probability of tumour eradication across a range of tumour burdens and mutational rates was estimated using mathematical modelling. Patient tumour burdens are several orders of magnitude higher than those used in mouse models and the mutational rate in patients with chronic-phase CML is likely to be markedly lower than the KCL-22 blast-phase CML cell line. Although difficult to estimate, it is thought that the mutation rate for genetically unstable cancer cells is more than 10^{-8}, whereas genetically stable cells range from 10^{-10} to 10^{-11} (refs 12, 15). The probability of tumour eradication using a combination of two agents with non-overlapping resistance compared to the scenario in which only a single agent is used was estimated. The probability of achieving complete tumour eradication is high ($P_{erad} = 1$ (blue)) across a range of tumour burdens and mutational rates when a combination of agents with resistance mechanisms that do not overlap are used (Fig. 3c). By contrast, the probability of tumour eradication is low ($P_{erad} = 0$ (red)) if only a single agent is used.

A phase I open-label, dose escalation trial evaluating ABL001 in patients with CML and Ph^+ ALL who were resistant or intolerant to at least two previous tyrosine kinase inhibitor (TKI) treatments is ongoing (ClinicalTrials.gov identifier: NCT02081378). Preliminary data in 35 patients receiving escalating doses revealed that ABL001 is well tolerated with dose-proportional pharmacokinetics. Most adverse events are grade 1 or 2, and the most common grade 3 or 4 adverse events are haematological cytopenias and increased levels of asymptomatic lipases[13]. Single-agent activity was noted at all dose levels tested (10–200 mg BID), with 11 out of 17 TKI-resistant patients achieving at least a 1-log reduction in BCR–ABL1 using the International Scale (IS) standardized baseline, and 5 achieving a major molecular response by 6 months[13]. Activity was seen across multiple TKI-resistant mutations and most patients remain on study. In total, 34 patients enrolled with chronic-phase CML, and 1 patient enrolled with accelerated-phase CML. This patient contained a Val299Leu mutation in BCR–ABL1 that emerged while on previous dasatinib therapy, and presented with a white blood cell count of 291×10^9 cells l^{-1} and 16% bone marrow myeloblasts. Single-agent treatment with ABL001 led to a complete haematological response by mid-cycle 2 and a complete cytogenetic response by cycle 3 (Fig. 4). However, the durability of the response was limited, and during cycles 4 and 5 resistant disease-containing myristoyl-site mutations Val468Phe and Ile502Leu emerged. To date, this is the only patient on study who has relapsed owing to the emergence of myristoyl-site mutations. This disease response profile mirrors many of the pre-clinical observations for ABL001 when dosed as a single agent. Notably, the activity against catalytic-site resistance mutations and the development of myristoyl-site point mutations strongly suggest that the anti-tumour activity seen in this patient resulted from the unique mechanism of action of ABL001 relative to currently approved TKIs.

ABL001 as a single agent induces clinical anti-tumour activity and is well tolerated to date in a heavily pre-treated subgroup of patients with

CML. Combinations of ABL001 with nilotinib, imatinib and dasatinib are now being explored in the phase I study to determine the recommended doses for future randomized clinical trials. These trials will probably focus on patients with early CML and test the hypothesis that a combination of ABL001 plus catalytic inhibitors will lead to disease eradication in a greater number of patients relative to single-agent treatments owing to improved overall responses and reduced rates of disease relapse.

The development of catalytic-site ABL1 kinase inhibitors such as imatinib has led to a shift in the treatment of patients with CML, with overall long-term survival exceeding 80%[1,16]. The development of second-generation ABL1 inhibitors led to faster, deeper responses predictive of superior outcomes[17–19]. Building on this initial therapeutic success, treatment is increasingly focused on a search for combination regimens with curative potential. Such regimens probably require three key characteristics: potency, tolerability and a low probability of acquired resistance. ABL001 has a similar potency profile to second-generation ABL1 inhibitors and by virtue of its myristoyl pocket binding exhibits an improved selectivity profile. Consistent with its unique mode of action, ABL001 displays a resistance profile distinct from that of catalytic-site inhibitors. The value of non-overlapping resistance profiles is evident in the combination efficacy studies showing durable treatment-free regressions in mouse models, and reinforced in simulations that model the probability of tumour eradication for clinically relevant tumour burdens. Once phase I testing has established safe combination doses of ABL001 with catalytic-site inhibitors, the potential for such combinations to achieve treatment-free remission in patients with CML can be tested.

Online Content Methods, along with any additional Extended Data display items and Source Data, are available in the online version of the paper; references unique to these sections appear only in the online paper.

Data Availability The authors declare that the data supporting the findings of this study are either available within the paper (and its Supplementary Information files) or are available from the corresponding author upon reasonable request.

Received 9 February 2016; accepted 7 February 2017.
Published online 22 March; corrected online 29 March 2017 (see full-text HTML version for details).

1. Kalmanti, L. *et al.* Safety and efficacy of imatinib in CML over a period of 10 years: data from the randomized CML-study IV. *Leukemia* **29,** 1123–1132 (2015).
2. Kantarjian, H. M., Baccarani, M., Jabbour, E., Saglio, G. & Cortes, J. E. Second-generation tyrosine kinase inhibitors: the future of frontline CML therapy. *Clin. Cancer Res.* **17,** 1674–1683 (2011).
3. Mahon, F. X. *et al.* Discontinuation of imatinib in patients with chronic myeloid leukaemia who have maintained complete molecular remission for at least 2 years: the prospective, multicentre Stop Imatinib (STIM) trial. *Lancet Oncol.* **11,** 1029–1035 (2010).
4. Ross, D. M. *et al.* Safety and efficacy of imatinib cessation for CML patients with stable undetectable minimal residual disease: results from the TWISTER study. *Blood* **122,** 515–522 (2013).
5. Adrián, F. J. *et al.* Allosteric inhibitors of Bcr-abl-dependent cell proliferation. *Nat. Chem. Biol.* **2,** 95–102 (2006).
6. Jahnke, W. *et al.* Binding or bending: distinction of allosteric Abl kinase agonists from antagonists by an NMR-based conformational assay. *J. Am. Chem. Soc.* **132,** 7043–7048 (2010).
7. Zhang, J. *et al.* Targeting Bcr-Abl by combining allosteric with ATP-binding-site inhibitors. *Nature* **463,** 501–506 (2010).
8. Hantschel, O. *et al.* A myristoyl/phosphotyrosine switch regulates c-Abl. *Cell* **112,** 845–857 (2003).
9. Nagar, B. *et al.* Structural basis for the autoinhibition of c-Abl tyrosine kinase. *Cell* **112,** 859–871 (2003).
10. Barretina, J. *et al.* The Cancer Cell Line Encyclopedia enables predictive modelling of anticancer drug sensitivity. *Nature* **483,** 603–607 (2012).
11. Manley, P. W. *et al.* Extended kinase profile and properties of the protein kinase inhibitor nilotinib. *Biochim. Biophys. Acta* **1804,** 445–453 (2010).
12. Bhang, H. E. *et al.* Studying clonal dynamics in response to cancer therapy using high-complexity barcoding. *Nat. Med.* **21,** 440–448 (2015).
13. Ottmann, O. G. *et al.* ABL001, a potent, allosteric inhibitor of BCR-ABL, exhibits safety and promising single-agent activity in a phase I study of patients with CML with failure of prior TKI therapy. *Blood* **126,** 138 (2015).
14. Tanaka, C. *et al.* Clinical pharmacokinetics of the BCR-ABL tyrosine kinase inhibitor nilotinib. *Clin. Pharmacol. Ther.* **87,** 197–203 (2010).
15. Kunkel, T. A. & Bebenek, K. DNA replication fidelity. *Annu. Rev. Biochem.* **69,** 497–529 (2000).
16. Al-Kali, A. *et al.* Current event-free survival after sequential tyrosine kinase inhibitor therapy for chronic myeloid leukemia. *Cancer* **117,** 327–335 (2011).
17. Marin, D. *et al.* Assessment of BCR-ABL1 transcript levels at 3 months is the only requirement for predicting outcome for patients with chronic myeloid leukemia treated with tyrosine kinase inhibitors. *J. Clin. Oncol.* **30,** 232–238 (2012).
18. Branford, S. *et al.* Prognosis for patients with CML and >10% BCR-ABL1 after 3 months of imatinib depends on the rate of BCR-ABL1 decline. *Blood* **124,** 511–518 (2014).
19. Hanfstein, B. *et al.* Early molecular and cytogenetic response is predictive for long-term progression-free and overall survival in chronic myeloid leukemia (CML). *Leukemia* **26,** 2096–2102 (2012).
20. Bozic, I. *et al.* Evolutionary dynamics of cancer in response to targeted combination therapy. *eLife* **2,** e00747 (2013).

Supplementary Information is available in the online version of the paper.

Acknowledgements The authors wish to thank the entire team who contributed to the discovery and development of ABL001.

Author Contributions A.A.W., J.D., W.Z., S.Bu., A.Q.H. and M.P. directed or performed cell signalling, enzymology and/or genetic characterization work. J.S., A.L.M. and X.P. directed or performed medicinal chemistry work. W.J., S.W.C.-J. and P.F. directed or performed structural biology, NMR and/or structural modelling and cheminformatics analysis. A.A.W., A.L., S.Bu., F.L., V.I., G.B., S.D. and S.T. directed or analysed *in vivo* pharmacology, pharmacokinetic, formulation and/or safety studies. H.B. performed mathematical modelling. K.G.V., S.Br., D.M.R. and T.P.H. were responsible for clinical strategy and/or investigations. L.P., M.W., F.H., N.J.K. and W.R.S. contributed to overall project oversight and strategy. A.A.W. and W.R.S. wrote the manuscript.

Author Information Reprints and permissions information is available at www.nature.com/reprints. The authors declare competing financial interests: details are available in the online version of the paper. Readers are welcome to comment on the online version of the paper. Publisher's note: Springer Nature remains neutral with regard to jurisdictional claims in published maps and institutional affiliations. Correspondence and requests for materials should be addressed to A.A.W. (andrew.wylie@novartis.com).

a

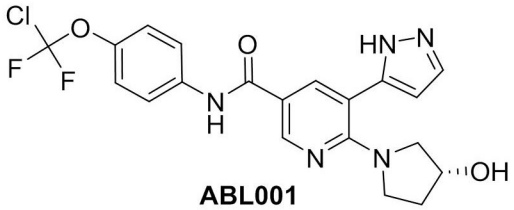

ABL001

b

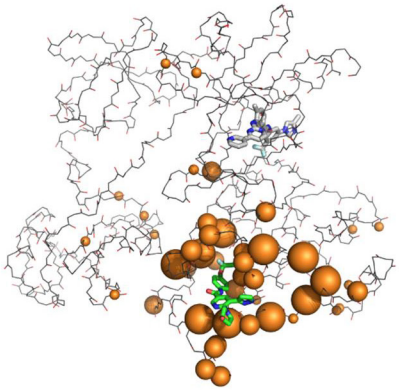

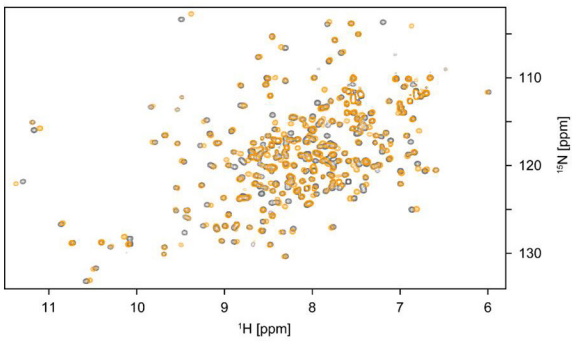

c

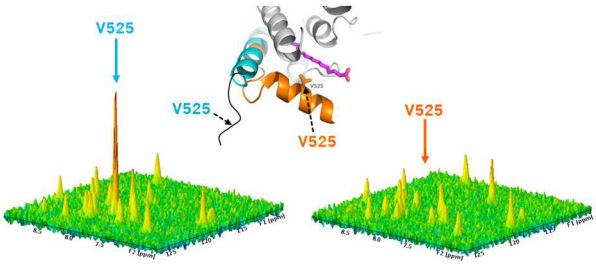

Unliganded Myr pocket

+ ABL001

d

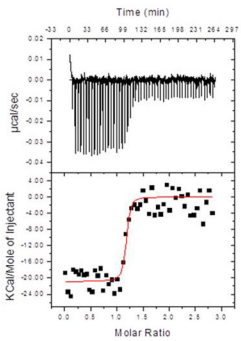

	K_A [M^{-1}]		K_D [nM]	N [mol/mol]	ΔH [kJ/mol]	ΔS [J/°C]
Exp. I	1.22E+09	± 70%	0.8	1.3	-20.8	-28.3
Exp. II	1.87E+09	± 39%	0.5	0.8	-18.3	-19.2

Extended Data Figure 1 | Chemical structure of ABL001 and biophysical characterization of its binding. a, Chemical structure of ABL001. **b**, NMR chemical shift assay to determine the location of ABL001 binding. **c**, NMR-based conformational assay using the resonance of Val525 to monitor the 'bending' of helix I in the presence and absence of ABL001. **d**, Isothermal calorimetry study to determine the binding affinity (K_a) of ABL001 to ABL1.

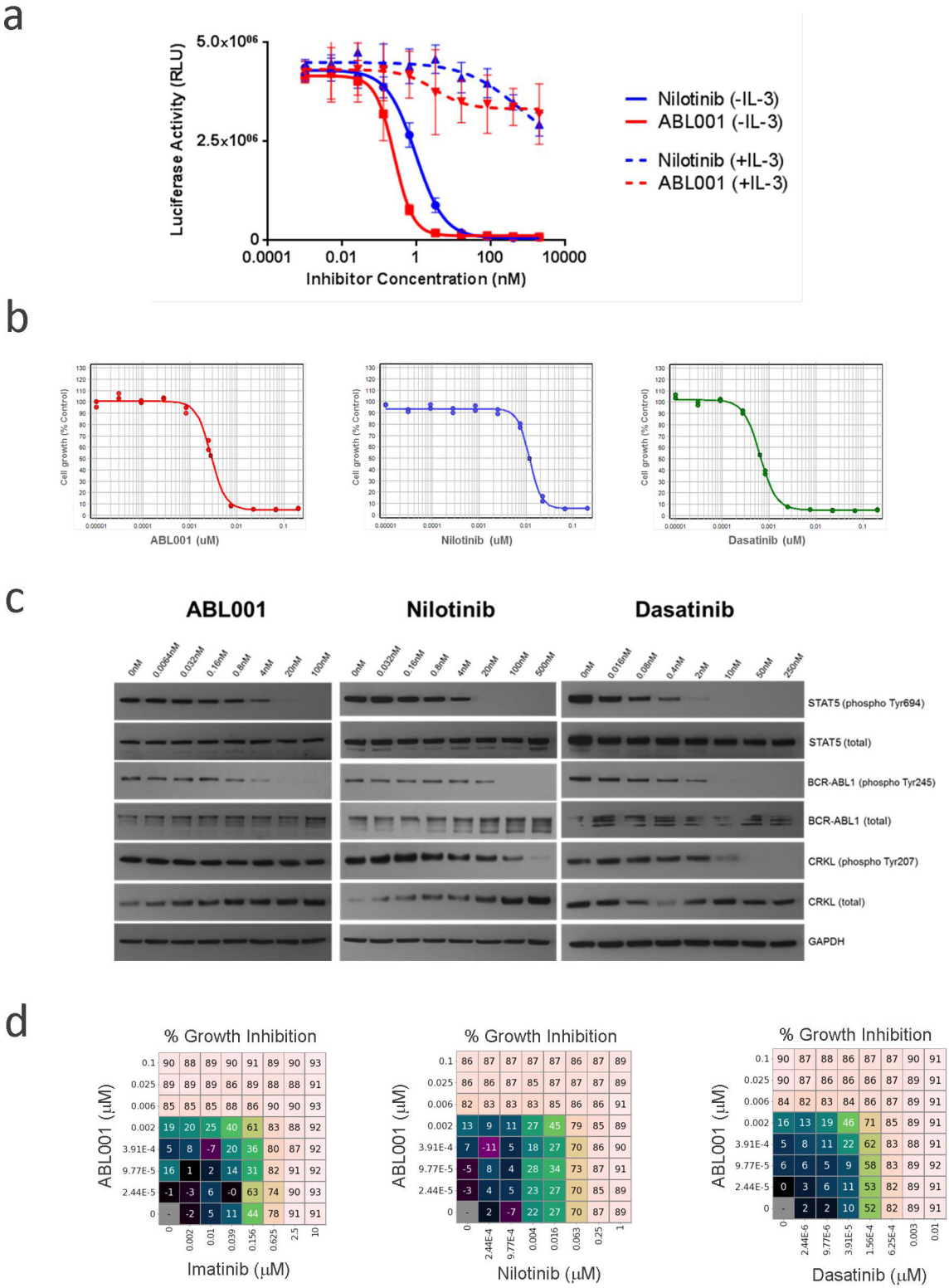

Extended Data Figure 2 | Cellular activity of ABL001 relative to catalytic inhibitors of ABL1. a, BCR–ABL1 48 h proliferation assay in Ba/F3 cells using a Britelite luciferase detection assay in the presence or absence of IL-3 across a dose range of ABL001 and nilotinib. Each assay was performed in quadruplicate; data are mean ± s.d. **b**, The sensitivity of KCL-22 cells to ABL001, nilotinib and dasatinib was determined in a 72-h growth assay. Each compound was tested in duplicate. **c**, KCL-22 cells were incubated with a range of compound concentrations for 1 h and immunoblots run to detect total STAT5 and pSTAT5 (Tyr694), total BCR–ABL1 and pBCR–ABL1 (Tyr245), total CRKL and pCRKL (Tyr207), and GAPDH as a loading control. **d**, Synergy studies were performed using ABL001 in combination with imatinib, nilotinib or dasatinib. KCL-22 cells were incubated with the compound combinations across a dose range for 72 h, and the level of cell growth relative to DMSO-treated cells was determined.

a

Mouse PK	
Dose IV	1 mg/kg (Solution*)
CL (mL/min/kg)	12
Vss (L/kg)	0.5
$t_{1/2term.}$ (h)	1.1
$AUC_{0\rightarrow\infty}$ (μM•h)	3.2
Dose PO	30 mg/kg (Solid dispersion**)
$AUC_{0\rightarrow\infty}$ (μM•h)	34
C_{max} (μM)	8
T_{max} (h)	2
Oral BA (%F)	35

Rat PK	
Dose IV	2 mg/kg (Solution*)
CL (mL/min/kg)	16
Vss (L/kg)	2.2
$t_{1/2term.}$ (h)	2.7
$AUC_{0\rightarrow\infty}$ (μM•h)	4.6
Dose PO	30 mg/kg (Solid dispersion**)
$AUC_{0\rightarrow\infty}$ (μM•h)	19
C_{max} (μM)	2.7
T_{max} (h)	4
Oral BA (%F)	27

Dog PK	
Dose IV	1 mg/kg (Solution*)
CL (mL/min/kg)	6
Vss (L/kg)	1
$t_{1/2term.}$ (h)	3.7
$AUC_{0\rightarrow\infty}$ (μM•h)	6.3
Dose PO	15 mg/kg (Solid dispersion**)
$AUC_{0\rightarrow\infty}$ (μM•h)	105
C_{max} (μM)	17
T_{max} (h)	0.8
Oral BA (%F)	111

* Solution dosing vehicle: 10% 1N HCl, 30% PEG300, 30(20%) Solutol, 10% 1N NaOH, 50mM acetate buffer pH 4.6
** Solid dispersion vehicle: 100% PBS

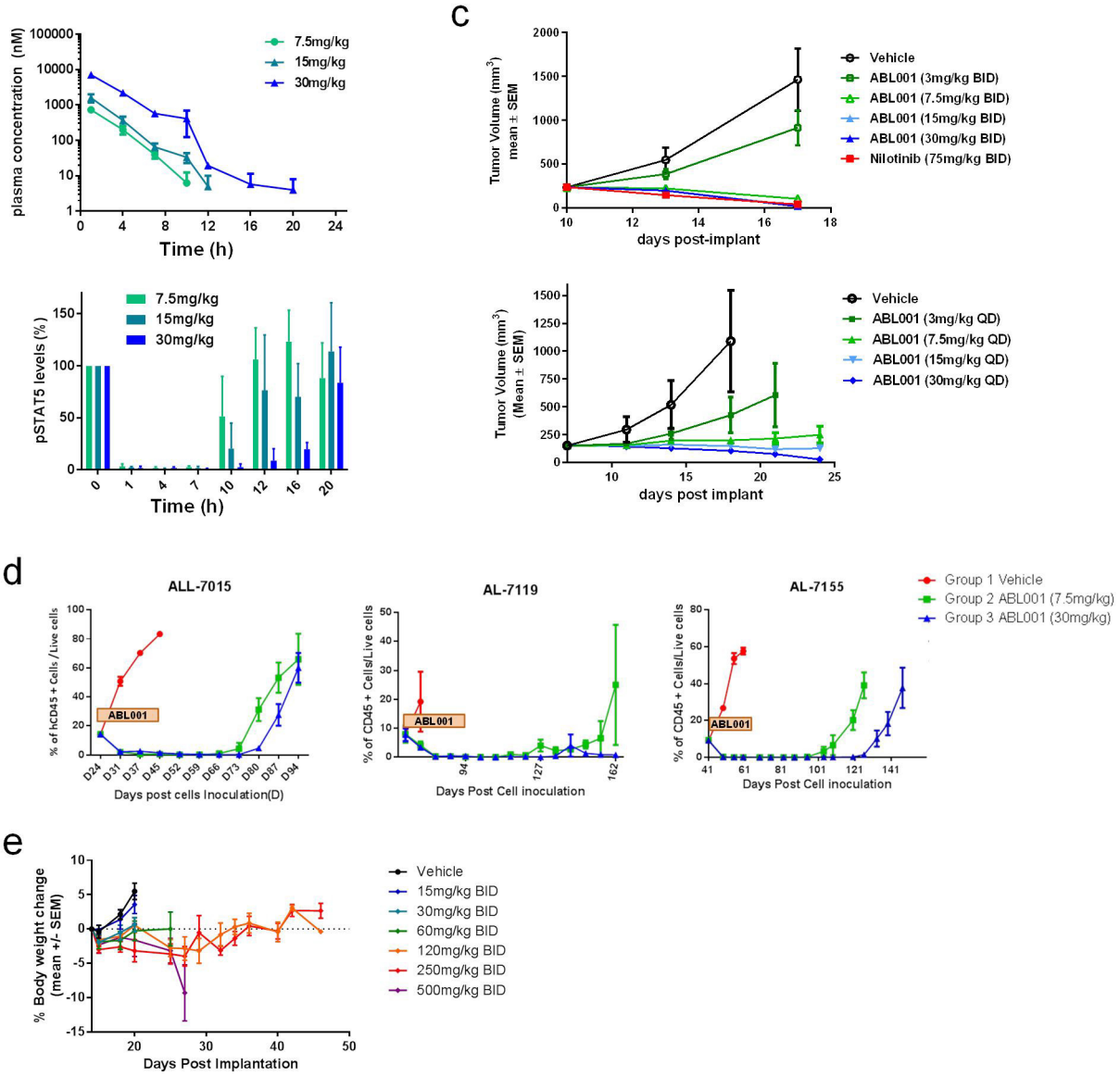

Extended Data Figure 3 | Pharmacokinetics, pharmacodynamics and efficacy of ABL001. a, Pharmacokinetic (PK) parameters of ABL001 in mouse, rat and dog after a single dose of ABL001. AUC, area under the curve; BA, bioavailability; CL, clearance; C_{max}, maximum concentration observed; IV, intravenous; $t_{1/2term}$, terminal half-life; PO, oral dosing; T_{max}, time at maximum concentration; Vss, volume of distribution. **b**, Total plasma concentrations and levels of pSTAT5 (Tyr694) in fine needle aspirate samples taken from KCL-22 xenografts were monitored after a single oral administration of ABL001 at doses ranging from 3 to 30 mg kg^{-1}. pSTAT5 (Tyr694) levels were determined using a pSTAT5 (Tyr694) meso scale discovery (MSD) assay with each sample run in duplicate; data are mean ± s.d. Samples are expressed as a percentage of the levels of pSTAT5 (Tyr694) before dosing ($t = 0$). **c**, ABL001 efficacy in KCL-22 xenograft tumours was assessed by monitoring tumour volume at doses ranging from 3 to 30 mg kg^{-1} on either a twice a day (BID) or once a day (QD) dosing schedules. Data are mean ± s.e.m. **d**, ABL001 efficacy in three patient-derived ALL systemic xenograft models (ALL-7015, AL-7119 and AL-7155) was assessed by FACS monitoring of the percentage of $CD45^+$ cells per live cell in blood samples taken at varying time points after dosing with either 7.5 mg kg^{-1} BID (group 2) or 30 mg kg^{-1} BID (group 3) ABL001 for 3 weeks. A control group (group 1) was treated with PBS vehicle. Data are mean ± s.e.m. ($n = 6$ per group). **e**, The tolerability of increasing doses of ABL001 dosed on a BID schedule was determined by monitoring mouse body weight 2–3 times per week. Data are mean ± s.e.m. ($n = 5$ per group).

a

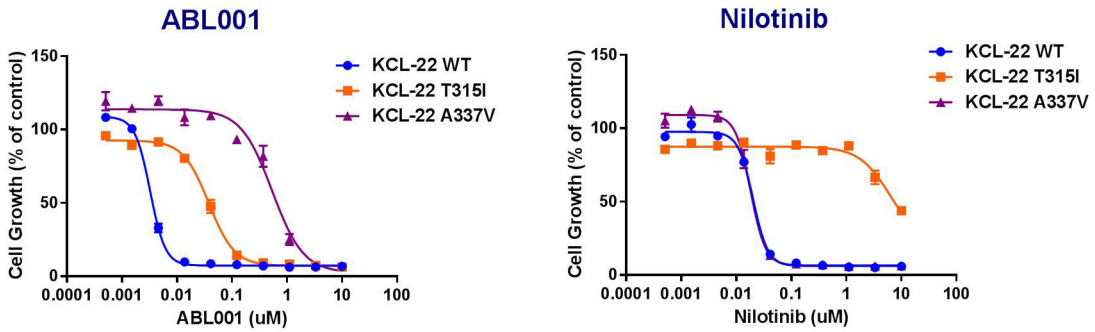

b

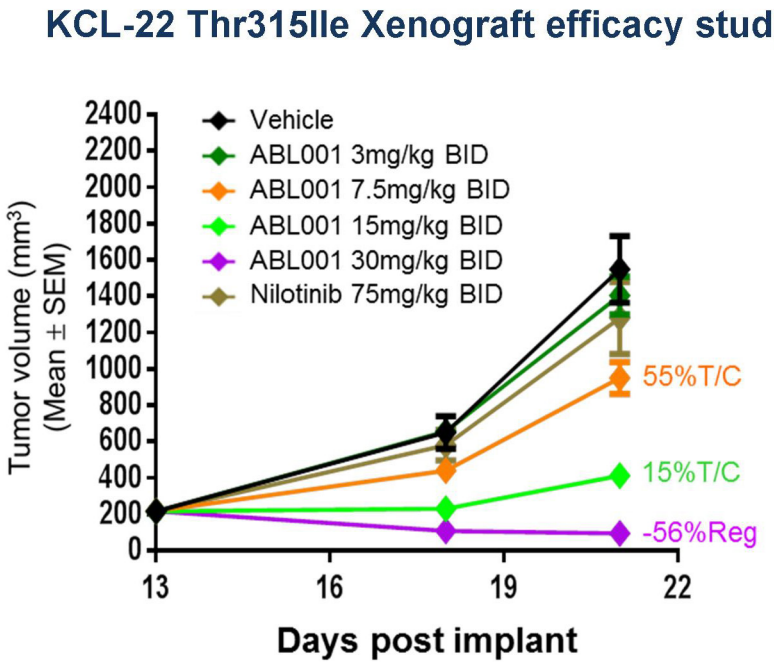

Extended Data Figure 4 | Activity of ABL001 and nilotinib in KCL-22 cell clones expressing Thr315Ile and Ala337Val BCR–ABL1 variants. **a**, The sensitivity of parental KCL-22 cells (WT) and KCL-22-resistant clones expressing BCR–ABL1 Ala337Val and Thr315Ile mutation variants to treatment with ABL001 (left) and nilotinib (right) was tested in 72 h growth assays. Samples were tested in duplicate; data are mean ± s.d. as a percentage of the vehicle-treated cells. **b**, KCL-22 Thr315Ile mutant cells were implanted as mouse xenografts and the efficacy of ABL001 across a dose range of 3–30 mg kg^{-1} BID was determined. Nilotinib was tested at 75 mg kg^{-1} BID as a control. Data are mean ± s.e.m. ($n = 7$ per group). T/C denotes ratio of tumour volume in control versus treated mice; 'Reg' denotes regression.

Extended Data Table 1 | Activity of ABL001 in biochemical assays

a

Kinase Assay	IC50 (uM)	Kinase Assay	IC50 (uM)
ABL1 (64-515)	0.00045	MAP3K7 (1-303) - TAB1 (437-	>10
ACVR1 (172-499)	>10	MAP3K8 (30-404)	>10
ADP-FRET PIK3CD	>10	MAP4K4	>10
ADP-FRET PIK3CG	>10	MAPK1	>10
AKT1	>10	MAPK10	>10
ALK (1066-1459)	>10	MAPK14	>10
AURKA	>10	MAPKAPK2	>10
BTK	>10	MAPKAPK5 (2-472)	>10
CAMK2D	>10	MET (956-1390)	>10
CDK1B	>10	MKNK1	>10
CDK2A	>10	MKNK2	>10
CDK4D1	>10	MTOR(1360-2549)	>10
CSK	>10	PAK2	>10
CSNK1G3 (35-362)	>10	PDGFRa (551-V561D-1089)	>10
EGFR (668-1210)	>10	PDPK1	>10
EPHB4 (566-987)	>10	PI3Ka	>10
ERBB4 (673-1308)	>10	PI3Kb	>10
FGFR1 (407-822)	>10	PI4Kb	>10
FGFR2 (406-821)	>10	PIM2	>10
FGFR3 (411-806)	>10	PKN1	>10
FGFR3 (411-K650E-806)	>10	PKN2	>10
FGFR4 (388-802)	>10	PLK1	>10
FLT3 (563-D835Y-993)	>10	PRKACA	>10
GSK3B	>10	PRKCA	>10
INSR (871-1343)	>10	PRKCQ	>10
IRAK1 (184-712)	>10	ROCK2 (6-553)	>10
IRAK4 (1-460)	>10	RPS6KB1 (1-421)	>10
JAK1 (866-1154)	>10	SRC (1-535)	>10
JAK2 (808-1132)	>10	STK17B	>10
KDR (807-1356)	>10	SYK (2-635)	>10
KIT (544-976)	>10	VPS34	>10
LCK (1-508)	>10	WNK1 (2-491)	>10
LYN (1-512)	>10	ZAP70	>10

b

Functional Assays	agonism IC50 (uM)	antagonism IC50 (uM)
5HT1A	> 30	> 30
5HT2A	> 30	17.5
5HT2B	> 30	5.9
Alpha 1A	> 30	> 30
Alpha 2A	> 30	> 30
Beta2	> 30	
CB1	> 30	> 30
D1	> 30	> 30
GABAA	29	> 30
H2	> 30	
M2	> 30	> 30
OpM	> 30	
rr AR	> 30	
ERalpha	> 30	> 30
GR		
PPARg	> 30	> 30
PR-B	> 30	13
PXR	> 30	> 30

Protease Assays	IC50 (uM)
hCaspase3 FLT	>100
hCathepsinD	>100
hMMP08	>100
hThrombin	>100

Assay	IC50 (uM)	Assay	IC50 (uM)
h Motilin	>30	5HT2C	>30
M1	>30	Ad1	>30
M3	>30	Ad2A	>30
op-delta	>30	Ad3	20.7
op-kappa	>30	alpha2B	>30
op-mu		alpha2C	>30
Y1	>30	beta1	>30
hr V1a	>30	AT1	29
hr V2	>30	B2	>10
r BzD	>30	CCKa	>30
r GABA A	>30	CCKb	>30
Nic(ns)	>30	D2	>30
r PCP	>30	D3	>30
5HT3	>30	ETa	>30
GR	>30	GHS	>30
AdT	26	H1	>30
DAT	>30	H3	>30
NET	22	MC3	>30
5HTT	>30		
ACES			
COX-1	>30		
COX-2	>30		
MAO-A	>30		
h PDE3	>30		
h PDE4D	>30		

a, Activity of ABL001 across a panel of kinase assays. **b**, Activity of ABL001 across a safety pharmacology panel of assays.